J. exp. Biol. (1977), 69, 87–105
With 13 figures
Printed in Great Britain

EFFECTS OF SEA ANEMONES ON THE FLOW FORCES THEY ENCOUNTER

BY M. A. R. KOEHL*
Department of Zoology, Duke University, Durham, North Carolina 27706

(*Received* 9 *December* 1976)

SUMMARY

Two species of sea anemones, *Metridium senile* and *Anthopleura xanthogrammica*, illustrate the sorts of compromises made by sessile organisms between maximizing the transport done and minimizing the mechanical forces caused by flow.

1. *M. senile* occur in calm areas, but because they are tall, they are exposed to mainstream current velocities. Although *A. xanthogrammica* occur in areas exposed to wave action, they are short and effectively hidden from mainstream velocities.

2. Measurements of drag forces on anemones and models in a flow tank and in the field indicate that the shapes, sizes, flexibilities, and behaviours of anemones affect the flow forces they encounter.

3. Although *M. senile* and *A. xanthogrammica* occur in different flow habitats, the drag force on an individual of either species is about 1 N.

4. The water currents encountered by these anemones and their mechanical responses to the currents can be related to the manner in which the anemones harvest food from flowing water.

INTRODUCTION

Organisms depending on moving fluid to transport them from place to place (such as various planktonic organisms or wind-dispersed seeds) have morphological features that maximize drag, whereas organisms that locomote through a fluid (such as birds or fish) tend to have structures that minimize drag. Sessile organisms (such as sea anemones or kelp) risk being dislodged or broken by drag forces, yet they depend on the fluid moving over them to bring them food and essential substances, to carry away their wastes, and to disperse their gametes or young.

Sessile organisms should therefore exhibit various compromises between minimizing and maximizing the effects of flow. I have investigated the ways in which the sizes, shapes and distributions of sessile animals affect the flow forces and feeding currents they encounter. There have been a number of studies of the distribution of benthic organisms in different types of flow (e.g. Southward & Orton, 1954; Ballantine, 1961; Gunjarova, 1968; Lewis, 1968; Hynes, 1970; Riedl, 1971; Schwenke, 1971), and a few biologists have actually measured flow velocities in the field (e.g. Charters, Neushul & Barilotti, 1969; Davies & Barham, 1969; Rhoads & Young,

* Present address: Friday Harbor Laboratories, Friday Harbor, Washington 98250.

1970; Grigg, 1972; Riedl & Machan, 1972; Terekhove, 1973), but the flow forces and the ways in which organisms affect them have not been investigated.

On the basis of the principles outlined below, I expected that the flow forces encountered by sessile animals would be determined by their structure and behaviour as well as by their locations in the environment. I made a comparative study of two species of sea anemones exposed to different flow conditions, the intertidal *Anthopleura xanthogrammica* (Brandt) (Fig. 1 C) which are found in areas exposed to extreme wave action (Rigg & Miller, 1949; Hand, 1955*a*; Ricketts & Calvin, 1968; Dayton, 1971), and the large subtidal individuals of *Metridium senile fimbriatum* (Verrill) (Fig. 1 A, B) which occur in areas exposed to tidal currents (Hand, 1955*b*; Ricketts & Calvin, 1968; Kozloff, 1973).

Some basic principles of the hydrodynamics of oscillatory flow

The flow force on a large organism in a tidal current when acceleration of the water is low (i.e. flow is essentially steady) can be estimated using the simple equation for drag at high Reynolds' number (Re),

$$F_D = \tfrac{1}{2}(C_D \rho\, U^2 S), \tag{1}$$

where C_D is an empirically determined drag coefficient that depends upon the shape of the object and the Re of the flow situation, ρ is the density of the fluid, U is the velocity, and S is the projected area of the body normal to the direction of flow (Rouse, 1961; Shapiro, 1961). Estimation of the flow forces on an organism in waves where water speed and direction rapidly change, however, is more complicated. Fortunately, ocean engineers have worked out a body of equations for predicting horizontal wave forces on pilings (high Re). A more thorough discussion of wave-induced forces can be found in Bascom (1964), Wiegel (1964), Carstens (1968), and Nagai (1973).

The water velocity during a wave cycle changes, hence the drag on a body in the wave changes. The drag (F_D) at any time (t) can be estimated using equation (1):

$$F_D(t) = \tfrac{1}{2} C_D \rho [U(t)]^2 S, \tag{2}$$

where $U(t)$ is the horizontal component of velocity at time t. Just as a greater force is needed to accelerate a body through a fluid than is needed to maintain the body at a constant speed, a greater force is exerted on a body over which fluid is accelerating than on the body over which fluid is moving at a constant speed. This extra acceleration force or inertial force (F_I), which is proportional to the horizontal component of the acceleration of the flow ($\dot{U}$) and to the mass of water displaced by the body ($\rho . V$), also changes with time (t) during the wave cycle;

$$F_I(t) = \tfrac{1}{4}\, C_M V \rho \dot{U}(t), \tag{3}$$

where C_M is the empirically determined coefficient of mass (dependent in part on the shape of the body) and V is the volume of the body. The C_D of an object in steady flow varies with Re, but the C_D and C_M of an object in oscillating flow tend to vary with another dimensionless number, the period parameter (P_p),

$$P_p = \frac{U_{\max} T}{D}, \tag{4}$$

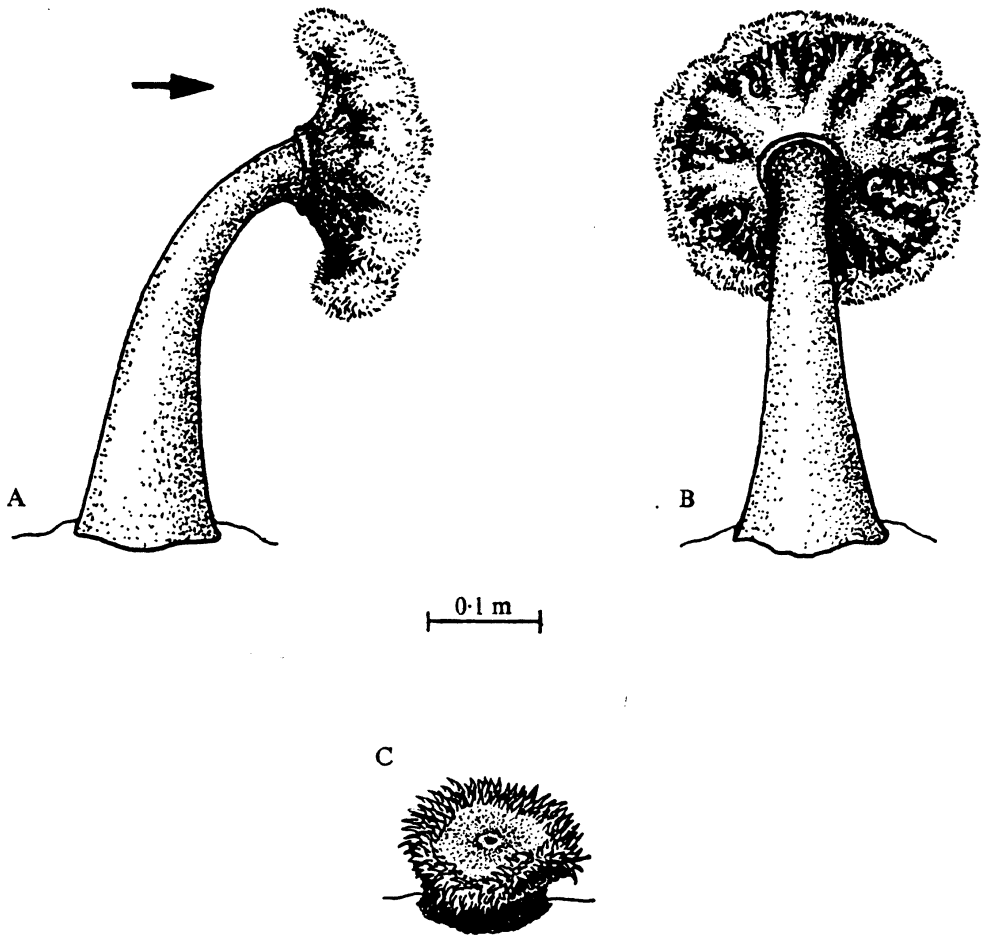

Fig. 1. A large subtidal *Metridium senile* bent over in a tidal current (arrow indicates flow direction). (A) Side view, (B) view from upstream (after Koehl, 1976); (C) an *Anthopleura xanthogrammica*.

where $U_{\max}$ is the maximum horizontal component of velocity attained during a wave cycle, T is the period of the wave, and D is the diameter of the object normal to the direction of flow (Keulegan & Carpenter, 1958). (There is, however, considerable scatter around Keulegan & Carpenter's (1958) curves of C_M or C_D against P_p of values measured in the field, thus various statistically derived values for C_D and C_M have also been suggested (Dean & Harleman, 1966; Agerschou, 1966).) The total force (F) on a body in a wave at time (t) is the sum of the drag (F_D) and the inertial force (F_I) at that time,

$$F(t) = F_D(t) + F_I(t). \tag{5}$$

Maximum F_D occurs when velocity reaches a maximum, but maximum F_I occurs at a different point during the wave cycle when acceleration is maximum. The maximum total force ($F_{\max}$) on an object during a wave cycle can be estimated by

$$F_{\max} = F_{D\max}\left[1 + \frac{1}{4}\left(\frac{F_{I\max}}{F_{D\max}}\right)^2\right], \tag{6}$$

when $0 \leqslant F_{I\,\max}/F_{D\,\max} \leqslant 2$, and by

$$F_{\max} = F_{I\,\max}, \tag{7}$$

when $F_{I\,\max}/F_{D\,\max} > 2$ (Bretschneider, 1966).

Although adequate for estimating flow forces, the above equations do not fully describe the complicated forces on bodies in waves. For example, they do not consider that the eddies formed behind a body move over it when flow direction is reversed. Nonetheless, these equations are very useful in that they describe the dependence of flow forces on a few basic measurable features of a body and the fluid moving around it.

Notation

C_D = drag coefficient
C_M = mass coefficient
D = diameter of a body normal to the flow direction
F_D = drag force
F_I = inertial force
$F(t)$ = total force on a body in a wave at time t
P_p = period parameter
Re = Reynolds' number = $(\rho UL)/\mu$, where L is a linear dimension of a body
S = projected area of a body normal to the direction of flow
T = period of a wave
U = velocity
$U(t)$ = horizontal component of velocity of water in a wave at time t
$\dot{U}(t)$ = horizontal component of acceleration of water in a wave at time t
V = volume of a body
μ = viscosity of a fluid
ρ = density of a fluid

Wave pressures

Sessile organisms in waves are subjected to pressure changes as well as to horizontal flow forces. The height of the water column above an organism, and hence the pressure on that organism, changes as a wave passes overhead, although such pressure changes are small. Larger pressures are exerted on shores by breaking waves. Large wave pressures ('shock pressures') last only a few thousandths of a second, are rare and cannot be predicted because their amplitude depends upon the particular shape and velocity of the wave and configuration of the shore at the moment of impact. It has been observed, however, that the pressures exerted on a shore by breaking waves are lower when air is entrained in the water, when the shore is horizontal or of gentle slope, and when the shore is cushioned by a layer of water such as the backwash of the previous wave (Wiegel, 1964: Carstens, 1968). I have not found *A. xanthogrammica* intertidally on exposed vertical rock walls normal to the direction of wave propagation where shock pressures are most likely to occur. Rather, I have found a few of these anemones on vertical walls parallel to the direction of wave propagation and many more on the horizontal bottoms of channels; these *A. xanthogrammica* are in the low intertidal zone where they are covered by a cushion of water when waves are breaking directly over them. I therefore do not

expect *A. xanthogrammica* to encounter large pressures due to breaking waves. Furthermore, an increase in pressure around an anemone filled with incompressible water would not subject it to a mechanical load unless it was in the pressure gradient at the edge of a shock pressure zone; such a pressure gradient would tend to push the anemone laterally. Because the probability of an *A. xanthogrammica* encountering such a gradient is low, I have restricted the present study to the horizontal drag and inertial forces that accompany each wave.

MATERIALS AND METHODS

By SCUBA diving and working low tides, I surveyed a number of sites along the coast of Washington to determine the characteristic habitats of *M. senile* and *A. xanthogrammica* and to observe their posturing and feeding behaviour. I assessed the shapes and dimensions of both species of anemones in the field as described in Koehl (1977).

I measured water velocities in order to characterize quantitatively the flow regimes of localities where the two species occur as well as of their microhabitats within those localities. With a thermistor flowmeter (LaBarbera & Vogel, 1976) capable of 1 mm spatial resolution, I was able to measure water speeds between the columns and tentacles of anemones. I used an electromagnetic flowmeter (EPCO Water Current Meter, Model 6130) to measure current velocities at exposed coastal sites. Flow probes were held rigidly in place by metal scaffoldings attached to the rock substratum in positions which did not interfere with the currents being measured. Simultaneous signals from both channels of either of the flow meters were recorded on CrO_2 magnetic tape using a portable stereo tape recorder (Sony TC-1261) and later transcribed using a chart recorder (Gould Brush 220) or an X–Y recorder (Hewlett-Packard, Model 7004B). The maximum standard error (S.E.) of repeated measurements transcribed in this way of the same velocity in a calibration tank was $\pm 3\%$ of the velocity for the electromagnetic flowmeter and $\pm 8\%$ for the thermistor flowmeter.

I constructed a force plate (Fig. 2) to make flow force measurements on anemones. Changes in resistance of X and Y strain gauges of the force plate were simultaneously monitored using two DC universal bridges (Bean, Model 101) and two strain meter-amplifiers (Bean, Model 502). Simultaneous signals from the two amplifiers were recorded and transcribed as described above. The force plate was calibrated by hanging weights from the specimen attachment point; the maximum standard error of repeated measurements of the same force recorded and transcribed as described was $\pm 5\%$. Anemones were allowed to attach to circles of plexiglas ($\frac{1}{4}$ in. thick) which were then affixed to the force plate. The force plate could be bolted to the rock substratum in the field as well as to the bottom of a flow tank (Vogel & LaBarbera, in preparation). Water velocities in the flow tank were measured by timing particles; the maximum standard deviation of repeated measurements of the same velocity was $\pm 8\%$. The flow tank was filled with Instant Ocean (33‰) and kept at 10 °C.

The contributions to drag of various aspects of the shape, texture and flexibility of the anemones, was tested by using the force plate to measure the drag on models of anemones in the field and in the flow tank. The models were made variously from clay, plaster, fabric, sheet aluminium, and flexible plastic foam.

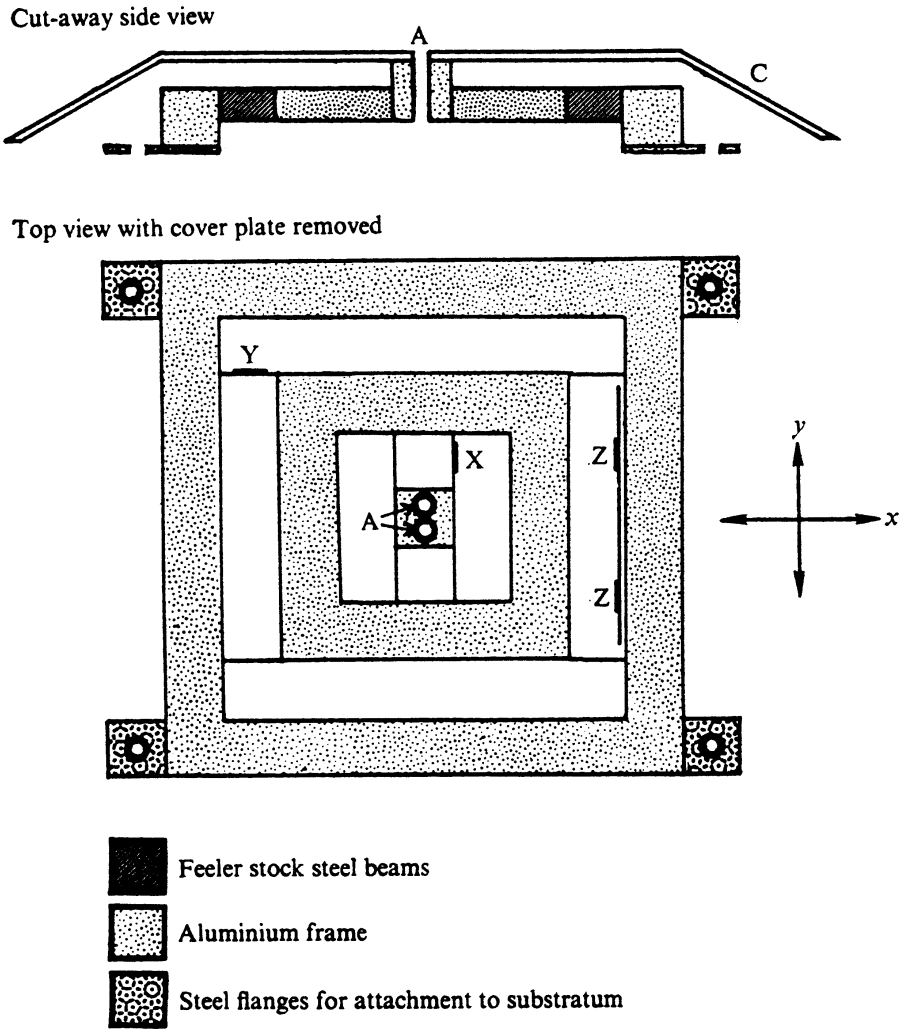

Fig. 2. Diagram of force plate. The bending of beam X is proportional to the component of force along the x axis and the bending of beam Y is proportional to the component of force along the y axis. The resultant of the x and y force vectors is the drag. Each of the beams is a $\frac{1}{2}$ in. wide strip of 0·012 in. gauge feeler stock steel (Precision Brand). The bending of each of the beams is measured by a foil strain gauge (Micro-Measurements, EA–06) affixed to the beam with RTC epoxy (Bean) and waterproofed with nitrile rubber (Bean Gagekote no. 2). Temperature-compensating strain gauges were affixed in the same manner to a feeler stock strip attached to the frame of the force plate with silicone sealant (Dow) so the strip would not be bent. A, points of attachment for cover plate and specimen; C, cover plate; X, strain gauge on beam X; Y, strain gauge on beam Y; Z, temperature-compensating strain gauges.

RESULTS AND DISCUSSION

Gross morphology and flow habitat

Along the Pacific coast of the United States, *Metridium senile* range from small, shallow-water animals with large tentacles, to large, deeper-water animals with lobed oral discs and numerous small tentacles (Hand, 1955*b*). I found the small *M. senile* in mussel beds at exposed coastal sites and on docks in Puget Sound, and the lobed large *M. senile* in the greatest abundance on vertical rock walls at depths greater than 10 m in Puget Sound. The few large *M. senile* along the outer coast were at

depths such that they did not experience the oscillating flow due to waves. The present study is limited to the lobed large *M. senile*.

The mean body proportions of expanded *M. senile* are reported by Koehl (1977). *M. senile* have long, slim, tapering columns topped by large, fluffy lobed oral discs. The most variable aspect of the shape of expanded *M. senile* is the diameter of the oral disc. *M. senile* are tall (mean height above substratum = 38·0 cm, standard deviation. S.D. = 9·0, $n = 28$). *M. senile* encounter steady tidal currents of relatively low velocity (the maximum velocities attained during the tidal cycles were less than 0·2 $m.s^{-1}$) (Fig. 3 B). The mean ratio of mainstream water velocity to velocity at the oral disc of *M. senile* was 1·02, to velocity at the upper column, 1·09, and to velocity at the lower column, 1·17; these ratios are not significantly different from each other, however ($F_{[2, 42]} = 1{\cdot}15$, $0{\cdot}25 < P < 0{\cdot}50$). Thus, because *M. senile* are tall, they are subjected to essentially mainstream current velocities (Fig. 3 C).

M. senile in flowing water are bent over (Figs. 1 A, B): this bending orients their oral discs normal to the water current. I have observed these anemones filtering zooplankton from the water passing through the meshwork of numerous small tentacles on their lobed oral discs. Gut content analyses confirm that *M. senile* are zooplanktivorous (Koehl, in preparation).

Anthopleura xanthogrammica commonly carpet the bottoms of intertidal surge channels at rocky exposed coastal sites. At high tide they are subjected to the oscillating bottom flow as waves pass overhead: at low tide they are subjected to the shoreward surge and seaward backwash of breaking waves. I also found a few solitary *A. xanthogrammica* at coastal sites where such wave action was attenuated by rock reefs located seaward of the anemones. The variance of the heights of *A. xanthogrammica* in exposed channels ((S.D.)^2 = 0·81) is significantly lower ($F_{[25, 71]} = 7{\cdot}11$, $P < 0{\cdot}002$) than the variance of the heights of *A. xanthogrammica* in protected areas ((S.D.)^2 = 5·76). The oral discs of *A. xanthogrammica* in groups carpeting exposed channels are all at essentially the same height; even though wider individuals tend to be taller (Fig. 4), wider anemones in exposed channels tend not to stand up taller than their narrower neighbours.

To assess whether the difference in height between exposed and protected *A. xanthogrammica* might be due to a structural difference between the two populations or to a transient difference in posture, I measured and collected individuals from both protected and exposed sites, put them in a sea table where flow velocity was < 0·05 $m.s^{-1}$, and measured their heights on the subsequent 8 days. The mean heights of exposed (2·1 cm) and protected (5·3 cm) *A. xanthogrammica* before they were collected were significantly different ($F_{[1, 13]} = 20{\cdot}63$, $P < 0{\cdot}001$), whereas after 8 days in the sea table they were not ($F_{[1, 11]} = 0{\cdot}59$, $P < 0{\cdot}50$). After 8 days in nearly still water, the anemones from protected sites had not changed significantly in height ($F_{[1, 6]} = 0{\cdot}04$, $P > 0{\cdot}75$), whereas the anemones from exposed channels were significantly taller ($F_{[1, 18]} = 7{\cdot}78$, $P < 0{\cdot}025$). This increase in height from a mean of 2·1 cm to a mean of 4·3 cm over a short period of time suggests that the difference in height between *A. xanthogrammica* from protected and exposed sites is due to posturing.

Current velocities over a shore are greatest during surge and backwash (Carstens, 1968). Mainstream flow in exposed surge channels during surge and backwash (Fig. 5 A, B) is bidirectional with a mean period of 7·7 s (S.D. = 0·9, $n = 37$). Because

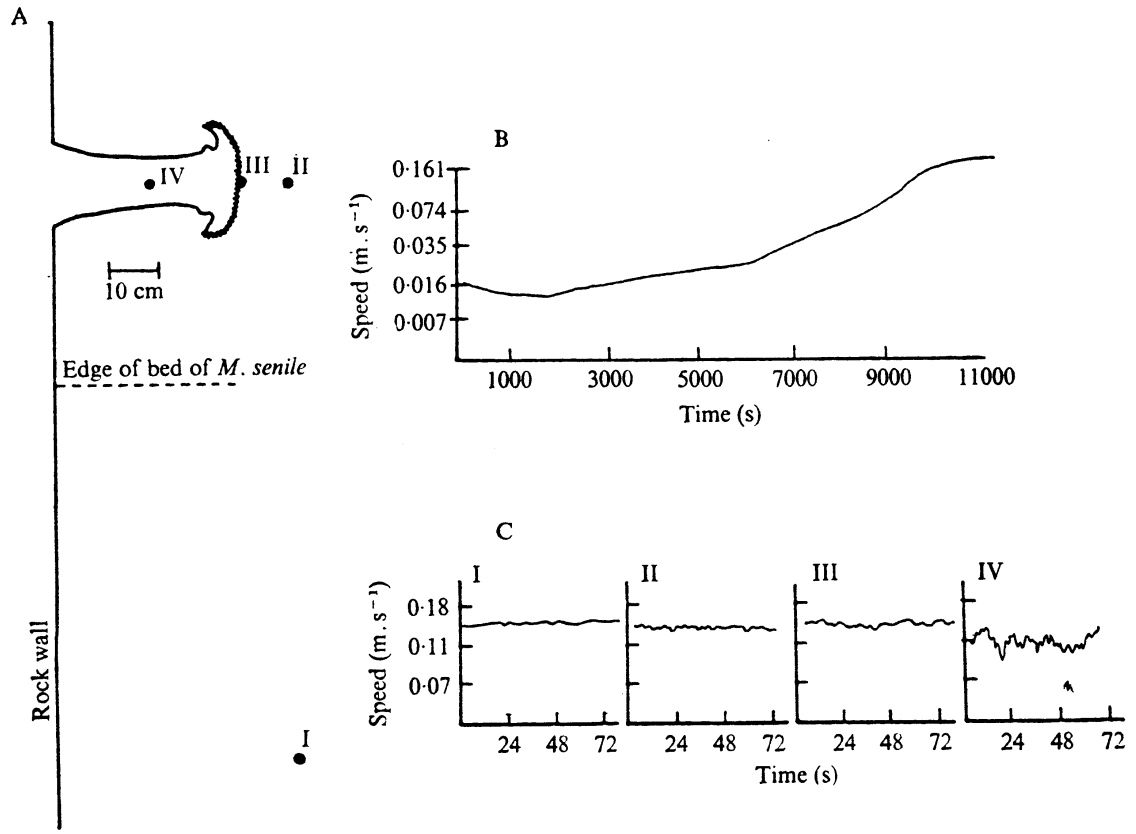

Fig. 3. Water speeds over *M. senile* measured by the thermistor flowmeter. (A) Diagram of a *M. senile* and the surrounding area indicating points (I–IV) where water speeds were measured. (B) Plot of water speed against time during part of the tidal cycle. (C) Plots of water speed measured at different points within a 15 min period. (Note that the water speed scale is logarithmic.)

A. xanthogrammica in exposed surge channels are so short, flow over these anemones is of lower velocity than mainstream (Figs. 5 C, D). Flow over the anemones is also more turbulent than mainstream. The mean of the maximum velocities of each wave surge 40 cm above the *A. xanthogrammica* in a surge channel (0·51 $m.s^{-1}$) is significantly ($F_{[1, 90]} = 174{\cdot}65$, $P < 0{\cdot}001$) faster than the mean of maximum velocities at their oral discs (0·21 $m.s^{-1}$). The variance of the maximum velocities 40 cm above the anemones $((S.D.)^2 = 0{\cdot}04)$ is significantly greater ($F_{[28, 111]} = 4{\cdot}0$, $P < 0{\cdot}002$) than that of maximum velocities at their oral discs $((S.D.)^2 = 0{\cdot}01)$, indicating that the flow microhabitat of the anemones is more constant than is the mainstream flow regime of the area where they occur. Mean maximum velocity of surge at different heights above an *A. xanthogrammica* in a surge channel and the mean velocity of tidal current above a *M. senile* on a vertical rock wall are plotted in Fig. 6. Unlike the tall *M. senile*, which encounter essentially mainstream flow, the short *A. xanthogrammica* 'hide' from the maximum flow velocities which characterize the areas where they occur.

In contrast, the taller *A. xanthogrammica* in protected areas stick out into mainstream currents. For example, the mean maximum velocity of surge 40 cm above an *A. xanthogrammica* at a protected site was 0·37 $m.s^{-1}$ (S.D. = 0·17, $n = 43$) and that at the oral disc of this anemone was also 0·37 $m.s^{-1}$ (S.D. = 0·17, $n = 154$); the variance

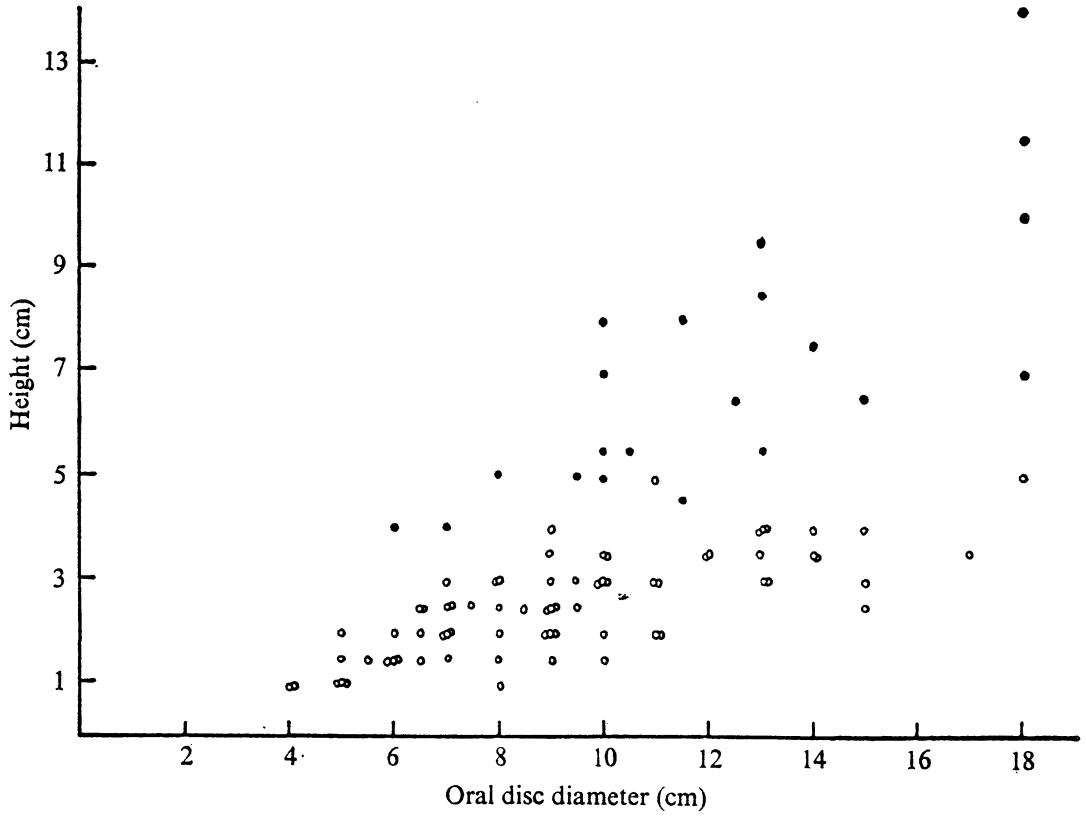

Fig. 4. Plot of the oral disc diameters and the heights of *A. xanthogrammica* from protected (●) and exposed (○) sites.

of maximum velocities ((S.D.)^2 = 0·3) is the same for mainstream flow and for flow on the anemones. Mean maximum surge velocity 40 cm above the oral discs of *A. xanthogrammica* at an exposed site (0·51 m.s^{-1}) was significantly faster ($F_{[1,123]}$ = 15·10, $P < 0{\cdot}001$) than that of a protected site (0·37 m.s^{-1}) measured within one hour on the same day. However, the mean maximum surge velocity on the oral discs of the 'protected' *A. xanthogrammica* (0·37 m.s^{-1}) is significantly faster ($F_{[1,263]}$ = 81·75, $P < 0{\cdot}001$) than that on 'exposed' anemones (0·21 m.s^{-1}) measured within that same hour. This illustrates that a knowledge of mainstream flow conditions does *not* tell us the flow regime encountered by a particular organism.

A. xanthogrammica feed primarily on mussels which fall on their oral discs after being ripped off the substratum by starfish, logs, and waves (Dayton, 1973). *A. xanthogrammica* do not visibly deform in flowing waters; they remain upright in surge and catch the large prey items such as mussels which settle out of the slower water eddying over the anemones (Koehl, in preparation).

Drag

Although *A. xanthogrammica* in exposed channels are hidden from mainstream currents and *M. senile* in calm areas are not, *A. xanthogrammica* encounters flow velocities generally two to four times higher than those met by *M. senile*. I therefore expected the structure of *A. xanthogrammica* to minimize drag more than that of

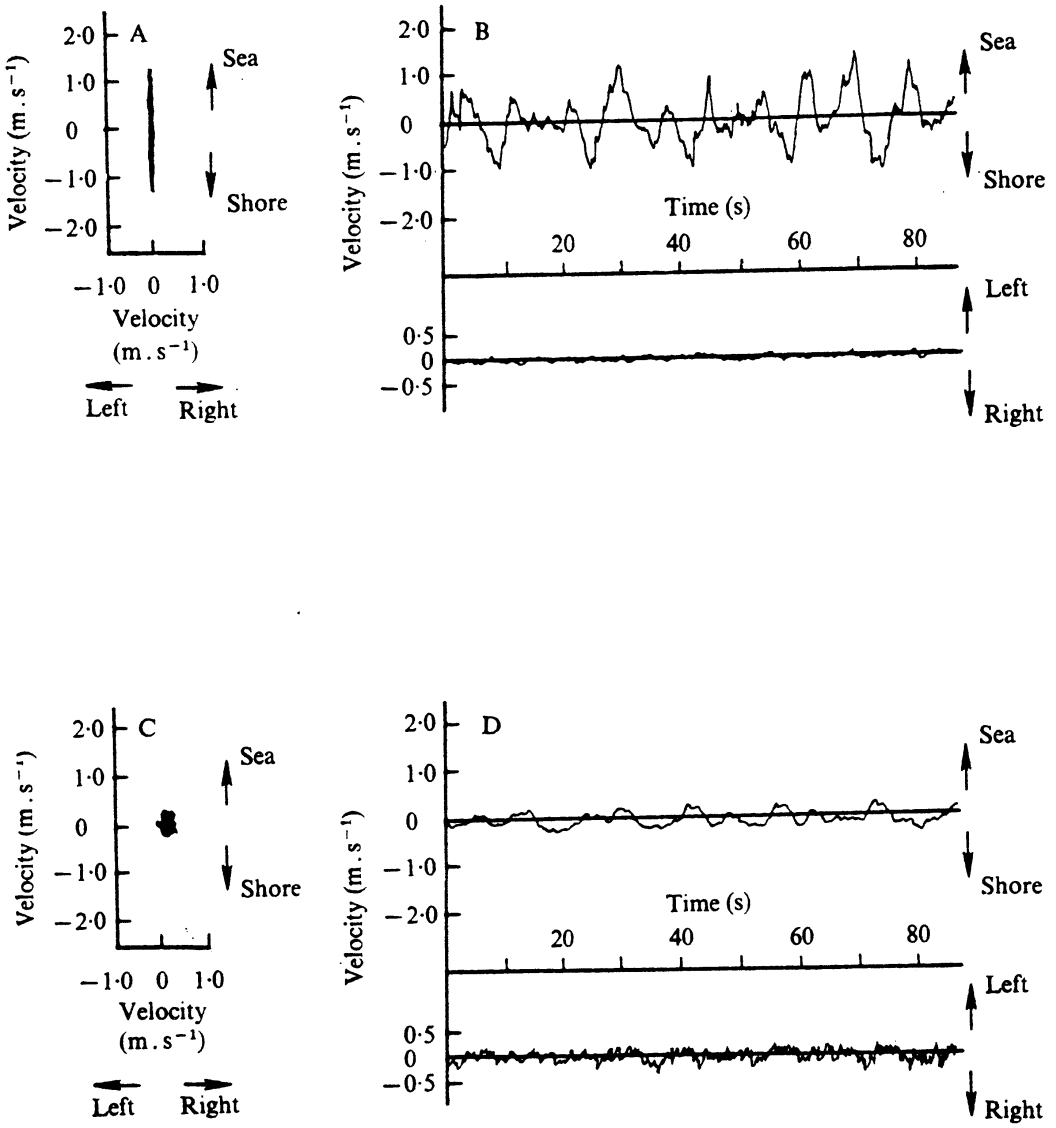

Fig. 5. Flow velocities measured by the EPCO 6130 flowmeter in a surge channel during surge and backwash. (A, B) Velocities 115 cm above the substratum. (C, D) Velocities 3 cm above the oral disc of an *A. xanthogrammica* surrounded by other *A. xanthogrammica* on the floor of the channel. In (A) and (C) velocity into ('shore') and out of ('sea') the channel is indicated on the vertical axis and flow from side to side ('right', 'left') in the channel is indicated on the horizontal axis. In (B) and (D) velocity (vertical axis) into and out of the channel and from side to side in the channel are both plotted against time (horizontal axis).

M. senile. The Re of a *M. senile* in a tidal current and the Re of an *A. xanthogrammica* in surge are both of the order of 10^4, hence pressure drag accounts for most of the drag on these anemones. Therefore, any shape, texture, or behaviour which minimizes wake size will minimize drag.

The flow forces on individual anemones were calculated using field measurements of their body dimensions and of flow velocities impinging on them. Each anemone was modelled as a combination of cylinders of the appropriate dimensions and the flow forces were computed as illustrated in the Appendix.

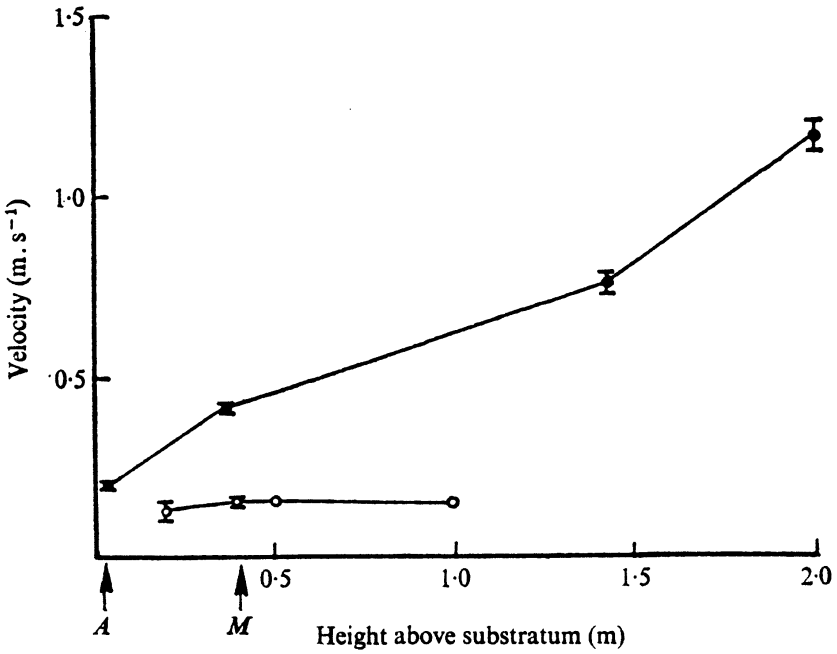

Fig. 6. Plot of mean maximum velocity (vertical axis) of wave surge at different heights (horizontal axis) above an *A. xanthogrammica* (●) in a surge channel (velocities were measured within a 30 min period during a low tide), and plot of mean velocity of tidal current at different heights above a *M. senile* (○) on a vertical rock wall (velocities were measured within a 10 min period during an incoming tide). Error bars indicate standard deviation. *A*, Height of the *A. xanthogrammica*; *M*, height of the *M. senile*.

The calculations of flow forces on specific anemones (Koehl, 1976) and on 'typical' anemones (Appendix I) indicate that although *M. senile* occur in calm regions and *A. xanthogrammica* in exposed areas, the flow force on an individual anemone of either species is nearly the same (about 1 N). I measured flow velocities over the anemones during the months of May, June, and July, 1975, and August, 1974, and no doubt velocities in surge channels during winter storms are higher than those I recorded. If the flow forces on exposed *A. xanthogrammica* are calculated (assuming they maintain the same shape during storms and assuming they encounter mainstream velocities) in a 'worst case' situation (Riedl (1972) reports 5 $m.s^{-1}$ as the maximum velocity attained in coastal channels), the forces are of the order of 20 N. This is probably an overestimate because the anemones can change their shapes and sizes and because they most likely are not exposed to mainstream currents.

To test how realistic these rough predictions of flow forces on anemones were, the force plate was used to measure force on an expanded *A. xanthogrammica* in an exposed surge channel where velocity and body dimension measurements had been made. The mean maximum force of wave surge on the force plate alone was significantly lower ($F_{[1,\ 80]} = 45{\cdot}57$, $P < 0{\cdot}001$, coefficient of determination = 0·36) than the mean maximum force on the plate plus the anemone. Hence the difference between mean maximum flow force on the plate plus anemone and on the plate alone, 1·2 N, is a reasonable estimate of the mean maximum force on the anemone. This estimate falls within the range of flow force values calculated for *A. xanthogrammica*.

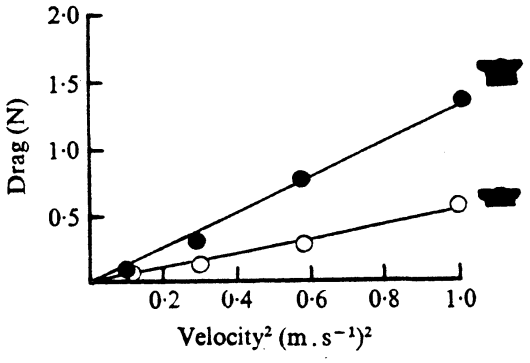

Fig. 7

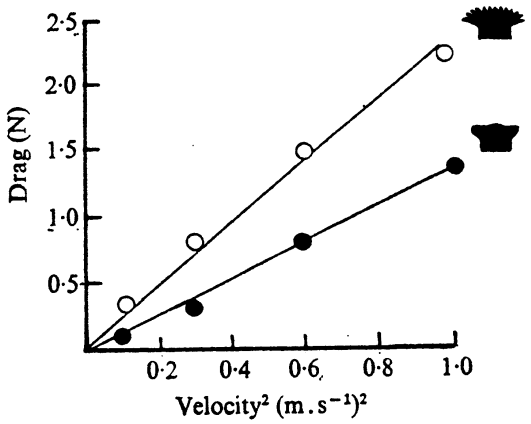

Fig. 8

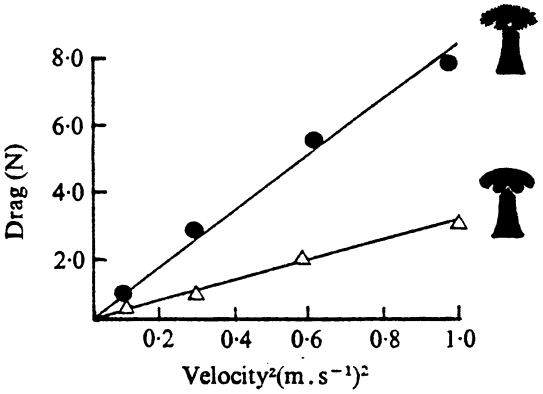

Fig. 9

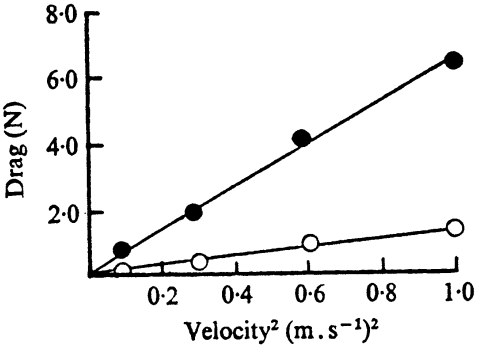

Fig. 10

Figs. 7–12. Graphs of drag against velocity². Values for C_D were calculated using equation (1). In some cases (e.g. Fig. 10) a model with higher drag has a lower C_D than a model with lower dragbecause the former presents more surface area normal to the flow direction ($C_D \propto 1/S$).

Fig. 7. A tall (●) (C_D = 0·3) and a short (○) (C_D = 0·2) model of an *A. xanthogrammica*.

Fig. 8. A model of an *A. xanthogrammica* with (○) (C_D = 0·7) and without (●) (C_D = 0·3) flexible tentacles.

Fig. 9. A model of a *M. senile* with (●) (C_D = 0·6) and without (△) (C_D = 0·1) flexible tentacles.

Fig. 10. A model of an *A. xanthogrammica* (○) (C_D = 0·6) with flexible tentacles and of a *M. senile* (●) (C_D = 0·2) bent over and with a flexible oral disc. The ratio of the projected area normal to the direction of flow to the projected area parallel to the direction of flow is roughly 1·0 for the *A. xanthogrammica* model and 2·5 for the *M. senile* model. Both models have a pedal disc diameter of 0·1 m.

I measured the drag on models of anemones in the flow tank at Re's between 10^4 and 10^5 to test the contributions of various aspects of shape, texture, and flexibility to drag. Drag was proportional to velocity² as would be expected for Re's of 10^4–10^5.

A tall anemone should experience greater drag forces than a short one of the same diameter for several reasons. As mentioned above, the taller the anemone, the less it is hidden in the slower moving fluid near the substratum. The tall anemone also has a larger projected area normal to the flow than does the short one. Furthermore, the larger a cylinder's ratio of diameter to length, the smaller the cylinder's C_D, because fluid flowing around the free end of the cylinder reduces the size of the wake behind

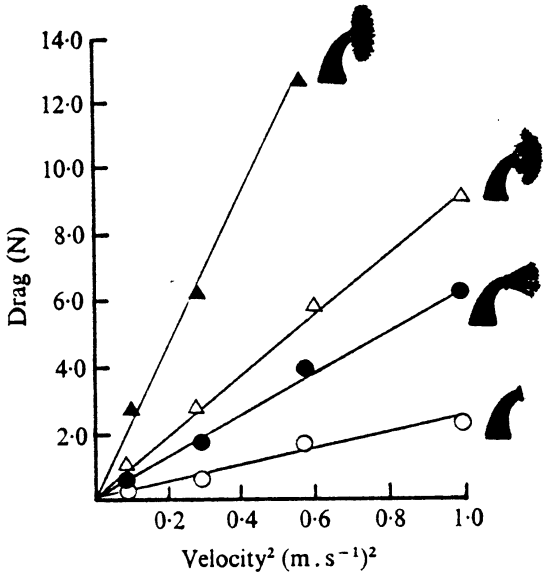

Fig 11.

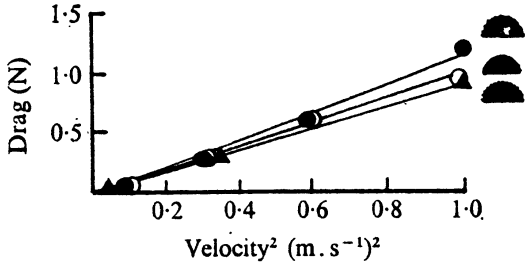

Fig 12.

Fig. 11. Models of bent *M. senile* with no oral disc (○) (C_D = 0·3), with a lobed flexible oral disc (●) (C_D = 0·2), with a lobed rigid oral disc (△) (C_D = 0·4), and with an un-lobed rigid oral disc (▲) (C_D = 0·9). All oral discs have flexible tentacles.

Fig. 12. A retracted *A. xanthogrammica* (●) (C_D = 0·4), a smooth model of a retracted anemone (○) (C_D = 0·4), and a model of a retracted anemone covered with soft verruca-like bumps (▲) (C_D = 0·4).

it (Rouse, 1961). The drag on a tall model of an *A. xanthogrammica* is greater than the drag on a shorter but otherwise identical model (Fig. 7). The ability of anemones to change their height thus enables them to modify the drag to which they are subjected.

An expanded anemone is not a plain cylinder, but has tentacles on its free end. It appears that tentacles make a large contribution to the drag on both *A. xanthogrammica* (Fig. 8) and *M. senile* (Fig. 9). Surge force measurements in the field for an *A. xanthogrammica* and for a model of the same dimensions, but without tentacles, indicated that mean maximum force on the anemone was 3·5 times greater than on the model.

Streamlined shapes minimize wake size, and thus pressure drag. A typical streamlined shape has a blunt nose and a long tapered tail. The rate of pressure increase along this tail is gradual and the point of boundary layer stall and separation occurs close to the rear tip of the body. The typical streamlined shape is effective in reducing drag only if the flow is from the blunt to the tapered end. It is therefore not surprising that organisms encountering unidirectional flow, such as fish and stream-bottom insect larvae, have the typical streamlined shape (Shapiro, 1961; Carstens, 1968; Hynes, 1970), whereas sessile organisms, such as anemones in tidal currents or waves where flow direction changes, do not. For a body in an area where flow direction changes, streamlining (i.e. minimizing the rate of pressure increase along a body in flow) may be accomplished to some degree by any shape or orientation which presents most of the exposed surface area of the body parallel to the direction of flow (this also reduces the projected area of the body normal to the direction of flow). Considered in these terms,

the shape of an *A. xanthogrammica* appears to be streamlined, whereas that of a *M. senile* bent over in flow with its oral disc normal to the direction of flow does not (Fig. 10). As expected, most of the drag on models of expanded *M. senile* is due to drag on the oral disc (Fig. 11). Drag measurements on models also indicate that because water can flow between the lobes of a *M. senile* oral disc, drag is lower than it would be if the oral disc were not lobed (Fig. 11).

When the flow velocity over a *M. senile* in the field is artificially increased, the flexible oral discs of these anemones collapse like an inside-out umbrella, which probably reduces drag. Drag measurements on models of *M. senile* with rigid and with flexible oral discs illustrate this effect (Fig. 11). Flexible *M. senile* in rapid flow are also bent down closer to the substratum where velocities, and thus drag forces, are lower. Thus, although the shape of a *M. senile* is far from being streamlined, the flexibility of these anemones offers a 'safety mechanism' whereby shape becomes more drag-minimizing as velocity increases, as has been shown for trees (Fraser, 1962). If the flow over a *M. senile* is artificially increased too much too abruptly, the anemone deflates and retracts into a hemisphere-shaped blob: this behaviour significantly reduces drag (compare Figs. 11 and 12).

Although a rough surface increases skin friction, it can sometimes reduce drag at high Re's by moving the point of boundary layer separation rearward on a body. If a fluid is moving rapidly over a rough surface, turbulence may be created in the boundary layer, therefore momentum can be transferred to the slower layers of fluid which are less likely to stall and cause separation (Shapiro, 1961). The columns of *A. xanthogrammica* are covered with wart-like bumps (verrucae) which may affect drag. I found, however, that drag on a verruca-covered model of a retracted *A. xanthogrammica* was nearly the same as the drag on a smooth model of the same dimensions (Fig. 12).

Compliant surfaces and polymer coatings on solid bodies have been found to reduce drag in many instances, although the exact mechanism of this effect is still being investigated (Kramer, 1965; Wells, 1969; Mordvinov, 1972; Cox, Dunlop & North, 1974; Virk, 1976). The soft surface and the mucous coating of a sea anemone may reduce drag. The drag measured on a soft, slimy *A. xanthogrammica*, however, was not noticeably different from that on a hard clean model of the same shape and dimensions (Fig. 12).

CONCLUSIONS

The shape, size flexibility, texture, and behaviour of an organism affects the flow forces it encounters, as illustrated by the sea anemones *M. senile* and *A. xanthogrammica*. *M. senile* occur in calm areas, but because they are tall, they are exposed to mainstream current velocities. Although *A. xanthogrammica* occur in areas exposed to wave action, they are short and effectively hidden from mainstream velocities. Nonetheless, water velocities encountered by *A. xanthogrammica* are greater than those met by *M. senile*. However, the drag force on an individual of either species is about 1 N due to the respective shapes of each species.

I have used the case of these two species of sea anemones to illustrate the sorts of compromises made by sessile organisms between maximizing the transport done and

minimizing the mechanical forces caused by flow. *M. senile* are distributed in areas where flow velocities are low, but have an array of morphological features that maximize the effects of the currents they do encounter. In contrast, *A. xanthogrammica* are distributed in areas where flow velocities are high, but have morphological features that minimize the effects of flow. The water currents encountered by these anemones and their mechanical responses to the currents can be related to the manner in which the anemones harvest food from flowing water. *M. senile* bend over in currents and suspension-feed through their oral discs whereas *A. xanthogrammica* remain upright in surge and catch mussels which fall on their oral discs.

This work was supported by a Cocos Foundation Training Grant in Morphology, a Graduate Women in Science Grant, a Sigma Xi Grant, and a Theodore Roosevelt Memorial Fund of the American Museum of Natural History Grant. I wish to express my appreciation to S. A. Wainwright whose support and feedback made this work possible, and to S. Vogel who introduced me to fluid mechanics and who gave me much helpful advice. I am grateful to R. Fernald and A. O. D. Willows for the use of facilities at Friday Harbor Laboratories, University of Washington. I thank the U.S. Coast Guard and R. T. Paine for making it possible for me to work on Tatoosh Island, and M. Denny, M. LaBarbera, K. Sebens, and T. Suchanek for their invaluable help in the field. I offer special thanks to M. LaBarbera for all his help with instrumentation, and to N. Budnitz for his advice on statistical analyses.

REFERENCES

AGERSCHOU, H. A. (1966). Fifth and first order wave-force coefficients for cylindrical piles. In *Coastal Engineering: Santa Barbara Specialty Conference, October* 1965, pp. 219–241. New York: American Society of Civil Engineers.

BALLANTINE, W. (1961). A biologically defined exposure scale for the comparative description of rocky shores. *Fd Stud.* 1, 1–19.

BASCOM, W. (1964). *Waves and Beaches, the Dynamics of the Ocean Surface.* Garden City, New York: Doubleday and Co., Inc.

BRETSCHNEIDER, C. L. (1966). The probability distribution of wave force and an introduction to the correlation drag coefficient and the correlation inertial coefficient. In *Coastal Engineering: Santa Barbara Specialty Conference, October*, 1965, pp. 183–217. New York: American Society of Civil Engineers.

CARSTENS, T. (1968). Wave forces on boundaries and submerged bodies. *Sarsia* **34**, 37–60.

CHARTERS, A. C., NEUSHUL, M. & BARILOTTI, C. (1969). The functional morphology of *Eisenia arborea*. *Int. Seaweed Symp.* **6**, 89–105.

CONNEL, J. H. (1970). A predator–prey system in the marine intertidal region. I. *Balanus glandula* and several predatory species of *Thais*. *Ecol. Monogr.* **40**, 49–78.

COX, L. R., DUNLOP, E. H. & NORTH, A. M. (1974). Role of molecular aggregates in liquid drag reduction by polymers. *Nature, Lond.* **249**, 243–5.

DAVIS, I. E. & BARHAM, E. G. (1969). An *in situ* surge-temperature recorder. *Limnol. Oceanogr.* **14**, 638–41.

DAYTON, P. K. (1971). Competition, disturbance, and community organization: the provision and subsequent utilization of space in a rocky intertidal community. *Ecol. Monogr.* **41**, 351–89.

DAYTON, P. K. (1971). Two cases of resource partitioning in an intertidal community: making the right prediction for the wrong reason. *Am. Nat.* **107**, 662–70.

DEAN, R. G. & HARLEMAN, D. R. F. (1966). Interaction of structures and waves. In *Estuary and Coastline Hydrodynamics* (ed. A. T. Ippen), pp. 341–403. New York: McGraw-Hill Book Co., Inc.

FRASER, A. I. (1962). Wind tunnel studies of the forces acting on the crowns of small trees. *Rep. For. Res., H.M.S.O. Lond.* 178–93.

GRIGG, R. W. (1972). Orientation and growth of sea fans. *Limnol. Oceanogr.* **17**, 185–92.

GUNJAROVA, E. (1968). The influence of water movements upon the species composition and distribution of the marine fauna and flora throughout the arctic and northern Pacific intertidal zones. *Sarsia* **34**, 83–94.

HAND, C. (1955*a*). The sea anemones of central California. II. The Corallimorpharian and Athenarian anemones. *Wasmann J. Biol.* **12**, 345–75.
HAND, C. (1955*b*). The sea anemones of central California. III. The Acontiarian anemones. *Wasmann J. Biol.* **13**, 189–251.
HYNES, H. B. N. (1970). *The Ecology of Running Waters*. Liverpool University Press.
KEULEGAN, G. H. & CARPENTER, L. H. (1958). Forces on cylinders and plates in an oscillating fluid. *J. Res. Natn Bur. Stan.* **60**, 423–40.
KOEHL, M. A. R. (1976). Mechanical design in sea anemones. In *Coelenterate Ecology and Behaviour* (ed. G. O. Mackie), pp. 23–31. New York: Plenum Publishing Corp.
KOEHL, M. A. R. (1977). Mechanical organization of cantilever-like sessile organisms: sea anemones. (Submitted to *J. exp. Biol.*)
KOEHL, M. A. R. Mechanisms of prey capture from flowing water by polyps. (In preparation).
KOZLOFF, E. N. (1973). *Seashore Life in Puget Sound, the Strait of Georgia, and the San Juan Archipelago*. Seattle: University of Washington Press.
KRAMER, M. O. (1965). Hydromechanics of the dolphin. *Adv. Hydroscience* **2**, 111–30.
LABARBERA, M. & VOGEL, S. (1976). An inexpensive thermistor flowmeter for aquatic biology. *Limnol. Oceanogr.* **21**, 750–6.
LEWIS, J. R. (1968). Water movements and their role in rocky shore ecology. *Sarsia* **34**, 13–36.
MORDVINOV, Y. Y. (1972). Effects of hair in some species of true seals (family Phocidae) on overall hydrodynamic drag. *Zool Zh.* **51**, 2–6.
NAGAI, S. (1973). Wave forces on structures. *Adv. Hydroscience* **9**, 254–324.
RHOADS, D. C. & YOUNG, D. K. (1970). Influence of deposit-feeding organisms on sediment stability and community trophic structure. *J. mar. Res.* **28**, 83–90.
RICKETTS, E. F. & CALVIN, J. (1968). *Between Pacific Tides*, 4th edn., revised by J. W. Hedgepeth. Stanford: Stanford University Press.
RIEDL, R. J. (1971). Water movement. In *Marine Ecology*, vol. I, Pt. 2 (ed. O. Kinne), pp. 1085–8, 1124–56. London: Wiley-Interscience.
RIEDL, R. J. & MACHAN, R. (1972). Hydrodynamic patterns in lotic intertidal sands and their bio-climatological implications. *Mar. Biol.* **13**, 179–209.
RIGG, G. B. & MILLER, R. C. (1949). Intertidal plant and animal zonation in the vicinity of Neah Bay, Washington. *Proc. Calif. Acad. Sci.* **26**, 323–51.
ROUSE, H. (1961). *Fluid Mechanics for Hydraulic Engineers*. New York: Dover Publications, Inc.
SCHWENKE, H. (1971). Water movement – Plants. In *Marine Ecology*, vol. 1, pt. 2 (ed. O. Kinne), pp. 1091–121. London: Wiley-Interscience.
SHAPIRO, A. H. (1961). *Shape and Flow: The Fluid Dynamics of Drag*. Garden City, New York: Doubleday and Co., Inc.
SOUTHWARD, A. J. & ORTON, J. H. (1954). The effects of wave action on the distribution and numbers of the commoner plants and animals living on the Plymouth breakwater. *J. mar. biol. Ass. U.K.* **33**, 1–19.
SVERDRUP, H. U., JOHNSON, M. W. & FLEMING, R. H. (1942). *The Oceans: Their Physics, Chemistry, and General Biology*. New York: Prentice-Hall, Inc.
TEREKHOVE, T. K. (1973). Effect of surf strength and current speed on the development of White Sea fucoid algae. *Hydrobiol. J.* **8**, 13–18.
VIRK, P. S. (1976). Conformational effects in drag reduction by polymers. *Nature, Lond.* **00**, 46.
VOGEL, S. & LABARBERA, M. A new water tunnel design for biological investigations. (In preparation).
WAINWRIGHT, S. A. & KOEHL, M. A. R. (1976). The nature of flow and the reaction of benthic cnidaria to it. In *Coelenterate Ecology and Behaviour* (ed. G. O. Mackie), pp. 5–21. New York: Plenum Press.
WELLS, C. S. (ed.) (1969). *Viscous Drag Reduction*. New York: Plenum Press.
WIEGEL, R. L. (1964). *Oceanographical Engineering*. Englewood Cliffs, New Jersey: Prentice-Hall, Inc.
ZERBE, W. B. & TAYLOR, C. B. (1953). Sea water density reduction tables. In *Coast and Geodetic Survey Special Publication*, no. 298, pp. 18–19. Washington, D.C.: U.S. Department of Commerce.

APPENDIX. SAMPLE CALCULATIONS OF FLOW FORCES ON SEA ANEMONES

Given: density (ρ) of sea water at 10 °C = 1026 kg.m^{-3} (Zerbe & Taylor, 1953); viscosity (μ) of sea water at 10 °C = $1{\cdot}39 \times 10^{-3}$ N.s.m^{-2} (Sverdrup, Johnson & Fleming, 1942).

(Water temperatures in areas along the coast of Washington where the anemones are found range from 5 to 16 °C (Connell, 1970).)

(A) *Force on a 'typical'* M. senile

I modelled a *M. senile* as diagrammed in Fig. 13A, thus

$$F_{D\ \text{total}} = F_{D\ \text{oral disc}} + F_{D\ \text{upper column}} + F_{D\ \text{lower column}}.$$

The dimensions of this 'typical' *M. senile* were calculated from the mean height of *M. senile* measured in the field ($\bar{x}$ = 0·38 m, S.D. = 0·09, n = 28) using the body proportions for *M. senile* listed in Table 1 of Koehl (1977). The flow velocities on the anemone were calculated for a mainstream velocity of 0·2 m.s^{-1} using the ratios, listed on page 93, of mainstream velocity to velocity at different heights on *M. senile*.

The Re for this *M. senile* was calculated using equation (1),

$$\text{Re} = \frac{(1026\ \text{kg.m}^{-3})(0{\cdot}20\ \text{m.s}^{-1})(0{\cdot}21\ \text{m})}{1{\cdot}39 \times 10^{-3}\ \text{N.s.m}^{-2}} = 3{\cdot}1 \times 10^{4}.$$

The acceleration of water over *M. senile* as the tidal current picks up is only of the order of 10^{-5} m.s^{-2}, thus I used equation (3) for the drag on a body in steady flow at high Re to calculate the flow force:

$$F_D = \tfrac{1}{2} C_D \rho U^2 S,$$

where C_D = 0·8 for a cylinder with a free end in steady flow at Re = 10^4 (Rouse, 1961), and where S = D.L for a cylinder. Thus,

$$\begin{aligned} F_{D\ \text{oral disc}} &= (0{\cdot}5)(0{\cdot}8)(1026\ \text{kg.m}^{-3})(0{\cdot}2\ \text{m.s}^{-1})^2\ (0{\cdot}201\ \text{m})(0{\cdot}107\ \text{m}) \\ &= 0{\cdot}37\ \text{N}, \\ F_{D\ \text{upper column}} &= (0{\cdot}5)(0{\cdot}8)(1026\ \text{kg.m}^{-3})(0{\cdot}18\ \text{m.s}^{-1})^2\ (0{\cdot}054\ \text{m})(0{\cdot}137\ \text{m}) \\ &= 0{\cdot}10\ \text{N}, \\ F_{D\ \text{lower column}} &= (0{\cdot}5)(0{\cdot}8)(1026\ \text{kg.m}^{-3})(0{\cdot}17\ \text{m.s}^{-1})^2\ (0{\cdot}084\ \text{m})(0{\cdot}137\ \text{m}) \\ &= 0{\cdot}14\ \text{N}, \end{aligned}$$

and

$$F_{D\ \text{total}} = 0{\cdot}61\ \text{N}.$$

(B) *Force on a 'typical'* A. xanthogrammica *in an exposed channel*

I modelled an 'exposed' *A. xanthogrammica* as diagrammed in Fig. 13B, thus

$$F_{\text{max total}} = F_{\text{max oral disc}} + F_{\text{max column}}.$$

The dimensions of this 'typical' exposed *A. xanthogrammica* were calculated from the mean height of exposed *A. xanthogrammica* ($\bar{x}$ = 0·025 m, S.D. = 0·009, n = 71) using the body proportions listed in Table 2 of Koehl (1977). The flow velocity used on the oral disc was the mean maximum velocity ($\bar{x}$ = 0·21 m.s^{-1}, S.D. = 0·12, n = 111) of surge recorded at the oral discs of exposed *A. xanthogrammica* during spring and summer months. The velocity on the column was calculated using the mean

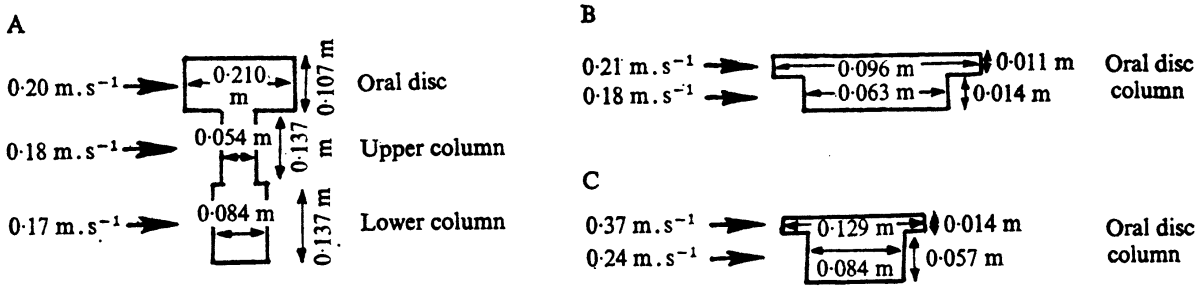

Fig. 13. Diagrams of 'typical' anemones in flow (heavy arrows). (A) a *M. senile*, (B) an *A. xanthogrammica* in an exposed surge channel, (C) an *A. xanthogrammica* in a protected site (explained in Appendix).

ratio I measured of column velocity to oral disc velocity ($\bar{x}$ = 0·87, S.D. = 0·09, n = 3) for exposed anemones. For each wave surge the maximum slope of a plot of velocity against time was taken as the maximum acceleration for that wave. The mean maximum acceleration at the oral discs of exposed *A. xanthogrammica* ($\bar{x}$ = 3·36 m.s^{-2}, S.D. = 1·95, n = 99) was used in these calculations. Since the period of wave surge at exposed sites ($\bar{x}$ = 7·8 s, S.D. = 0·9, n = 37) was the same on columns and oral discs, the acceleration on the column was estimated as 0·87 of that on the oral disc.

The Re for maximum velocity flow on this *A. xanthogrammica* was calculated using equation (1),

$$\mathrm{Re} = \frac{(1026\ \mathrm{kg.m^{-3}})(0{\cdot}21\ \mathrm{m.s^{-1}})(0{\cdot}096\ \mathrm{m})}{1.39 \times 10^{-3}\ \mathrm{N.s.m^{-2}}} = 1{\cdot}5 \times 10^{4}.$$

Since this anemone in surge represents a high Re oscillating flow situation, the maximum drag force was calculated using equation (2) and the maximum inertial force using equation (3),

$$F_{D\ \max} = \tfrac{1}{2} C_D \rho U_{\max}^{2} S,$$

and

$$F_{I\ \max} = \tfrac{1}{4} C_m \rho \dot{U}_{\max} \pi D^2 L.$$

The P_p's for the oral disc and for the column were calculated using equation (4).

$$P_{p\ \text{oral disc}} = \frac{(0{\cdot}21\ \mathrm{m.s^{-1}})(7{\cdot}8\ \mathrm{s})}{0{\cdot}096\ \mathrm{m}} = 17, \text{ and}$$

$$P_{p\ \text{column}} = \frac{(0{\cdot}18\ \mathrm{m.s^{-1}})(7{\cdot}8\ \mathrm{s})}{0{\cdot}063\ \mathrm{m}} = 22,$$

hence, $C_{D\ \text{oral disc}}$ = 1·8, $C_{m\ \text{oral disc}}$ = 0·9, $C_{D\ \text{column}}$ = 1·6, and $C_{m\ \text{column}}$ = 1·0 (Keulegan & Carpenter, 1958). Thus, for the oral disc,

$$F_{D\ \max} = (0{\cdot}5)(1{\cdot}8)(1026\ \mathrm{kg.m^{-3}})(0{\cdot}21\ \mathrm{m.s^{-1}})^2\ (0{\cdot}011\ \mathrm{m})$$
$$= 0{\cdot}04\ \mathrm{N}, \text{ and}$$

$$F_{I\ \max} = (0{\cdot}25)(0{\cdot}9)(1026\ \mathrm{kg.m^{-3}})(3{\cdot}36\ \mathrm{m.s^{-2}})(3{\cdot}14)(0{\cdot}096\ \mathrm{m})^2\ (0{\cdot}011\ \mathrm{m})$$
$$= 0{\cdot}24\ \mathrm{N},$$

and for the body,

$$F_{D\ \max} = (0{\cdot}5)(1{\cdot}6)(1026\ \mathrm{kg.m^{-3}})(0{\cdot}18\ \mathrm{m.s^{-1}})^2\ (0{\cdot}063\ \mathrm{m})(0{\cdot}014\ \mathrm{m})$$
$$= 0{\cdot}02\ \mathrm{N},$$

and

$$F_{I\,\max} = (0{\cdot}25)(1{\cdot}0)(1026\ \text{kg.m}^{-3})(2{\cdot}92\ \text{m.s}^{-2})(3{\cdot}14)(0{\cdot}063\ \text{m})^2\ (0{\cdot}014\ \text{m})$$
$$= 0{\cdot}13\ \text{N}.$$

Thus,

$$F_{D\,\text{max total}} = 0{\cdot}06 \quad \text{and} \quad F_{I\,\text{max total}} = 0{\cdot}37.$$

Since

$$\frac{F_{I\,\text{max total}}}{F_{D\,\text{max total}}} = 6{\cdot}17 > 2, \quad F_{\text{max total}} = 0{\cdot}4\ \text{N}.$$

(C) *Force on a 'typical'* A. xanthogrammica *in a protected site.*

I modelled a 'protected' *A. xanthogrammica* as diagrammed in Fig. 13C.

The dimensions of this 'typical' protected *A. xanthogrammica* were calculated from the mean height of protected *A. xanthogrammica.* ($\bar{x}$ = 0·07 m, S.D. = 0·02, n = 25) and using the body proportions listed in Table 2 of Koehl (1977). The flow velocity used on the oral disc was the mean maximum velocity ($\bar{x}$ = 0·37 m.s^{-1}, S.D. = 0·17, n = 154) of surge recorded at the oral disks of protected *A. xanthogrammica* during spring and summer months. The velocity on the column was calculated using the mean ratio of column velocity to oral disc velocity ($\bar{x}$ = 0·68, S.D. = 19, n = 5) for protected anemones. The mean maximum acceleration at the oral discs of protected *A. xanthogrammica* ($\bar{x}$ = 4·38 m.s^{-2}, S.D. = 2·62, n = 118) was used in these calculations, and the acceleration on the column was estimated to be 2·98 m.s^{-2}. The period of wave surge in protected areas ($\bar{x}$ = 1·10 s, S.D. = 1·8, n = 15) was used in calculating P_p.

The Re for maximum velocity flow in this *A. xanthogrammica* was calculated to be $3{\cdot}5 \times 10^4$, thus the flow forces were calculated in the same manner as they were for the 'exposed' *A. xanthogrammica* above. The calculated $F_{\text{max total}}$ was 2·84 N.